crystals

MDPI

Article

The Performance Prediction of Electrical Discharge Machining of AISI D6 Tool Steel Using ANN and ANFIS Techniques: A Comparative Study

Hamed H. Pourasl [1,*], Mousa Javidani [2,*], Vahid M. Khojastehnezhad [1] and Reza Vatankhah Barenji [3]

[1] Department of Mechanical Engineering, Cyprus International University, TRNC, Via Mersin 10, Nicosia 99258, Turkey; vkhojasteh@ciu.edu.tr
[2] Department of Applied Science, University of Québec at Chicoutimi, Saguenay, QC G7H 2B1, Canada
[3] Department of Engineering, School of Science and Technology, Nottingham Trent University, Nottingham NG11 8NS, UK; reza.vatankhahbarenji@ntu.ac.uk
* Correspondence: hpourasl@ciu.edu.tr (H.H.); mousa_javidani@uqac.ca (M.J.)

Abstract: AISI-D6 steel is widely used in the creation of dies and molds. In the present paper, first the electrical discharge machining (EDM) of the aforementioned material is performed with a testing plan of 32 trials. Then, artificial neural networks (ANN) and adaptive neuro-fuzzy inference system (ANFIS) were applied to predict the outputs. The effects of some significant operational parameters—specifically pulse on-time (Ton), pulse current (I), and voltage (V)—on the performance measures of EDM processes such as the material removal rate (MRR), tool wear ratio (TWR), and average surface roughness (Ra) are extracted. To lead the process operators, process plans (i.e., parameter–effect correlations) are created. The outcomes exposed the upper values of pulse on-time caused by higher amounts of MRR and Ra, and likewise lower volumes of TWR. Furthermore, growing the pulse current resulted in upper volumes of the material removal rate, tool wear ratio, and surface roughness. Besides, the higher input voltage resulted in a lower amount of MRR, TWR, and Ra. The estimation models developed by using experimental data recounting MRR, TWR, and Ra. The root means the square error was used to determine the error of training models. Furthermore, the estimated outcomes based on the models have been proven with an unseen validation set of experiments. They are found to be in decent agreement with the experimental issues. The investigation shows the powerful learning capability of an ANFIS model and its advantage in terms of modeling complex linear machining processes.

Keywords: electrical discharge machining; artificial neural network (ANN); ANFIS; AISI D6 tool steel; tool wear ratio (TWR); MRR

Citation: Pourasl, H.H.; Javidani, M.; Khojastehnezhad, V.M.; Vatankhah Barenji, R. The Performance Prediction of Electrical Discharge Machining of AISI D6 Tool Steel Using ANN and ANFIS Techniques: A Comparative Study. *Crystals* **2022**, *12*, 343. https://doi.org/10.3390/cryst12030343

Academic Editor: Heinz-Günter Brokmeier

Received: 29 January 2022
Accepted: 25 February 2022
Published: 2 March 2022

1. Introduction

The difficulty in treating hard-to-cut materials impacted the start of numerous progressive machining approaches such as water jet machining, electric discharge machining, laser machining, and electrochemical machining. These processes, commonly termed non-traditional machining procedures, create energy to remove residual material from the stock to create the preferred portion. Of these procedures, electric discharge machining (EDM) has received ample attention from the nuclear, aerospace, and automobile subdivisions [1]. Regardless of the extraordinary price of the apparatus (e.g., electron beam processing, water jet, and laser) or the disadvantage of dangerous slope (e.g., electrochemical machining), it is still superior to other methods. The electrode modeling tool has a shape that is the opposite of the cut profile. The additional material is censored through a sequence of sparks among the tool and the workpiece in the form of a dielectric medium that works as an insulator to avoid the material declaration reserved externally to the device. The EDM procedure has

found numerous uses such as fabrication of molds/dies and the cutting of holes in a variety of materials containing metals and composites [2] by vast distance to diameter ratio.

Various research has attempted to improve the quality attributes of the EDM process through a change in the process parameters. Boujelbene et al. [3] inspected the outcome of energy ignition on the tool wear ratio (TWR), material removal rate (MRR), and the depth of altered layer (i.e., the material re-solidified on the work-surface) in the machining of two steels: X200Cr15 and 50CrV5. They described the depth of the altered layer and the augmented MRR and the obstinately condensed TWR as the sparking energy was enlarged. Pradhan et al. [4] considered the performance of copper and aluminum electrodes on the EDM of EN-8 steel to display that the copper electrode executed better in terms of outward value. Besides, they found that the surface quality declined with a rise in the pulse-on-time (200 µs to 700 µs) over the reflected range of peak current (8 A to 24 A). Amorim et al. [5] examined the effect of polarized graphite and copper electrodes on the EDM performance of AISI P20 steel. As demonstrated by the outcomes, advanced MRR was achieved when the dispensation was prepared with the graphite electrode but good surface quality was appreciated when machining was approved with the copper electrode. Jefferson et al. [6] suggested that application of cryogenic usage on the electrode could improve the surface quality of the work piece.

Bhupinder Singh and J.P. Misra [7] used RSM and ANN modeling to study the apparent finish investigation of electric wire discharge machined samples through. This research determined the optimal morals of factors for the WEDM of nickel-based super alloys that will offer options to engineering production and to machine tool workers depending upon their occupation necessities. Vishnu P et al. [8] worked on the presentation forecast of electric discharge machining of inconel-718 by ANN. They used backpropagation algorithms to forecast performance characteristics, specifically MRR, SR, and TWR.

Tebni et al. [9] detected the influence of the difference in the pulse current, pulse on-time, and pulse off-time on the surface quality, MRR, and altered layer depth on two steels (50CrV4 and X200Cr15). They offered to work with a weak current pulse with short time if the surface quality was mainly neutral, and they consistently chose high sets of these factors if production speed was the main objective. Moreover, in order to reduce the depth of the replaced layer, low saving of input energy was proposed. The same results have been noted in the literature on 40CrMnNiMo864 steel [10]. Muthuramalingam and Mohan [11] observed the influence of a discharge current on machinability in EDM to show that the adapted ISO pulse achieved better surface quality than the prepared predictable pulse.

Chandramouli et al. [12] closely studied the outcome of MRR, TWR, and Ra by using input properties such as pulse-off time, current, and pulse-on time. Kibra et al. [13] described the outcome of diverse dielectrics on MRR, TWR, over-cut, and surface reliability during the micro-EDM of Ti-6Al-4V with a tungsten electrode. Retaining a copper electrode, Jeykrishnan et al. [14] operated on EN24 tool steel, optimizing procedural factors and expending the Taguchi technique. Yongfeng et al. [15] investigated an experimental study of EDM factors for zrb2-sic ceramics machining, and they discussed the effect of EDM factors on ZrB2-SiC ceramics EDM machining technique.

Employing a Cu-W electrode, Marafona [16] optimized the model through the design of an experimental approach. Guo and Tsai [17], using a genetic algorithm, developed an optimum model for processing BaTiO semi-conductive material. Shrivastava and Dubei [18] performed an intelligent modeling and multi-objective optimization of electric discharge diamond grinding. Baraskar et al. [19] applied a mixture of the genetic algo1ritm and the response surface methods to optimize the EDM of EN8 steel. Ramesh Raju et al. [20] worked on optimizing process parameters in the electrical discharge machining of haste alloy C276 using Taguchi's method. In this investigation, an attempt was made to determine the optimum process variables for obtaining better machining performance in terms of the material removal rate and the surface roughness. Basha et al. [21] worked on the experimental study of electrical discharge machining of Inconel X-750 using a tungsten-copper electrode. The results showed that the MRR increased with an increase in the

discharge current and pulse on-time, and the lower surface roughness was obtained at the initial conditions of the discharge current and pulse-on time.

Tsai and Wang [22] have proven that besides processing parameters, the material's physical properties such as heat conductivity, specific heat capacity, boiling point, melting point, and electrical conductivity play an essential role in determining the performance of the EDM process. From this research, it is understandable that EDM process performance is highly dependent on the material used. Thus, the setup parameters that are optimal for performance tend to vary between test materials. Therefore, a search should be made for each of the responsible parameters for each material.

Rajesh and Gagandeep [23] have investigated the effects of process parameters on the performance of electrical discharge machining of AISI M42 high-speed tool steel alloy. The objective of the study was to determine the effect of machining parameters on MRR such as the current, tool polarity, pulse on-time, and gap voltage for AISI M42 alloy. Singh et al. [24] instigated a mathematical model to predict MRR during gas-based EDM.

Khalid Al-Ghamdi and Osman Taylan [25] conducted a comparative study on modeling the material removal rate by ANFIS and on polynomial methods in the electrical discharge machining process. The results for this study showed that the ANFIS model with 21 rules was the best. Singh et al. [26] worked on predictive analysis of surface roughness in EDM using semi-empirical, ANN, and ANFIS techniques. In this research, a mathematical model was actuated to realize the SR by utilizing dimensional analysis hypothesis. Bobbili et al. [27] completed a comparative report on the wire electric discharge machining of materials used in defense for making arms with the dimensional method related to MRR and SR. In other investigations, Singh and Singh [28] put forward a mathematical model to estimate SR during gas-based EDM. Their findings revealed that the developed model predicted the responses with agreeable accuracy.

The AISI-D6 steel offers excellent corrosion resistance and high toughness at elevated temperatures. Thus, it is used extensively in the making of forming dies and injection molds. However, due to its high hardness, it is not an easy process to cut through typical mechanical machining. Therefore, different solutions with no mechanical machining means are to be used. In this study, the EDM process is used to cut AISI-D6 steel. To investigate the needed parameters offering the optimal performance, some essential input parameters—namely pulse on-time, pulse current, and voltage—are varied over tests. Their output effects such as MRR, TWR, and Ra are recorded. The drawn process maps provide guidelines for understanding the process users for quality EDM of AISI-D6 material. Moreover, adaptive neuro-fuzzy inference system (ANFIS) and artificial neural network (ANN) machine-learning approaches have been applied to the output estimation of the parameters. The control variables used for MRR, TWR, and Ra are pulse current, pulse on-time, and voltage.

2. Experimental Procedure

2.1. Work-Piece and Tool

The material for the electrode tool used for the EDM process needs to be electrically conductive. There is a wide range of materials that can be used to manufacture electrodes such as graphite, electrolytic copper, brass, tungsten carbides, silver-tungsten alloy, copper tungsten alloys, tellurium-copper alloys, and copper-graphite alloys. For the present study, an electrode made of electrolytic copper with a machining interface of 18 mm diameter and the AISI-D6 tool steel hardened to 60 HRC were, respectively, employed as the electrode and experimental materials. The test pieces and electrodes were precisely machined to the sizes given in Table 1 and Figure 1.

Table 1. Tool and work-piece specifications.

Material	Type	Length (mm)	Diameter (mm)
Tool	Copper	20	18
Work-piece	AISI D6	20	20

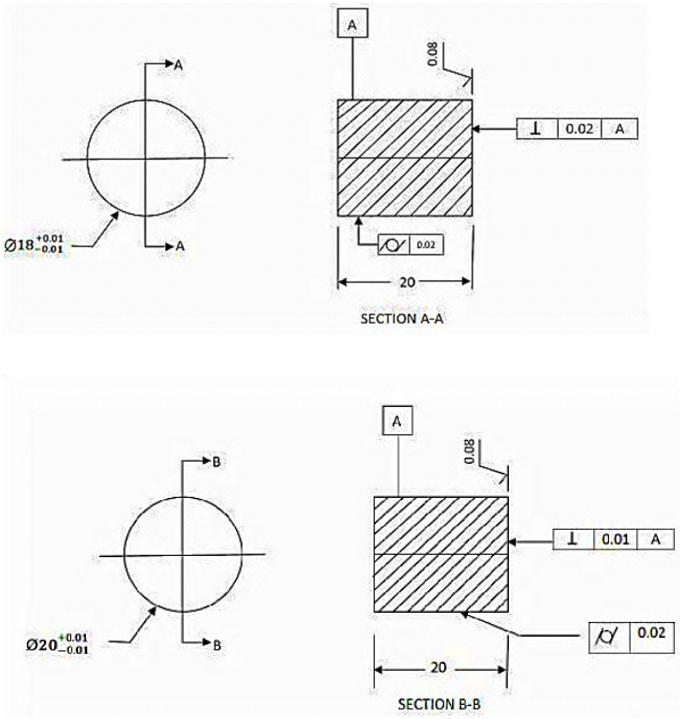

Figure 1. Tool and work-piece specifications.

2.2. Experimental Setup

Table 2 shows the parametric conditions for conducting the experimental trials. The controlling parameters pulse on-time (Ton) and pulse current (I) each was varied over four levels. The steel was usually cut in the range of 150 V to 250 V [29,30]; therefore, this specific parameter was varied over only two levels so that the number of tests could be minimized. The other parameters were set as: machining gap = 2 mm; duty cycle = 20; and polarity = positive. Kerosene oil was used as the dielectric medium. A three-level full-factorial experiment comprising 4 × 4 × 2 = 32 runs was conducted. In all, 32 experiments, as listed in Table 2, were performed on the Azarakhsh Ayzvpals CNC EDM system shown in Figure 2.

Table 2. Parametric conditions for conducting the experimental trials.

Parameters	Units	Notations	Levels			
			1	2	3	4
Discharge current	A	I_P	8	10	12	14
Pulse on-time	µs	T_{On}	10	20	30	40
Discharge voltage	Volt	V	150	250	-	-
Dielectric used			Kerosene oil			
Dielectric flushing			Side flushing with pressure			
Work material			AISI D6 steel			
Electrode material			Electrolytic pure copper			
Electrode polarity			Positive			
Work material polarity			Negative			

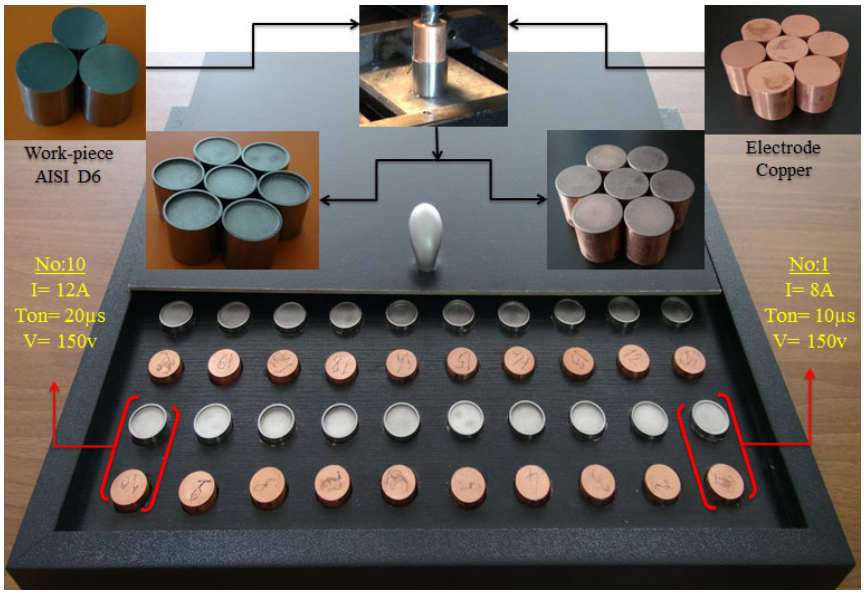

Figure 2. On-job process and samples produced through EDM.

2.3. Performance Measures in EDM

After the completion of every testing scenario, the relative output characteristics, such as MRR, TWR, and Ra were measured. The MRR and TWR weighing process was done by checking the difference in the masses of steel and copper tools before and after use in the machining process using a digital precision scale Mettler Toledo AB265 with an accuracy of ±0.00001 g. The MRR in mm^3/min and TWR in g/g were calculated employing the following relationships:

$$MRR = \frac{(M_{W1} - M_{W2})}{(P_W \times t)} \times 10^3 \quad (1)$$

$$\%TWR = \frac{(M_{T1} - M_{T2}) \times P_W}{(M_{W1} - M_{W2}) \times P_T} \times 100 \quad (2)$$

where MRR is the material removal rate; and TWR is the tool wear ratio. The weight of workpiece (in grams) before and after machining are M_{W1}, M_{W2}, and M_{T1}, M_{T2} are the weight of tool (in grams) before and after machining. The density of the workpiece in g/cm^3 is ρ_W; t is the machining time in minutes; and ρ_T is the density of the Cu tool (i.e., 93.8 g/cm^3).

3. Result and Discussion

In experimental applications, the effect of the input parameters on the output performance of electronic discharge machining differs from theory. Thus, it is recommended to set the I and the T_{on} to high values and the voltage to low values if productivity is the prime objective during the electronic discharge machining of AISI-D6 steel. However, contrarily, the T_{on} and the I need to be set to high values and the voltage must be kept low when the tool wear ratio is the major objective. To obtain less surface roughness, low values for the pulse on-time and the pulse current and large values for the voltage are recommended.

3.1. Machine Learning Algorithms

Machine learning is a branch of artificial intelligence. In this research, artificial intelligence teaches computers to do what a human operator may do, i.e., regressive learning. As the learning samples increase, the algorithm's performance improves adaptively [31]. Deep learning began from artificial neural networks which is a subcategory of machine learning. Machine learning usually implements neural network-based operations such as deep learning. The application of deep learning is available in all industries from automated driving to medical devices [32]. Wuest, Weimer, Irgens & Thoben (2016) distinguished the supervised

and unsupervised machine learning algorithm. Supervised machine learning was suitable for most manufacturing applications mainly because manufacturing applications provided labeled data [33].

Machine learning (ML) applications are used in all areas of industry. Machine learning approaches are implemented in procedural compliance, documentation of process and orientation, and risk and quality frameworks in the manufacturing industry. Machine learning is utilized in cloud computing, data science, and IoT. The ability of machine learning approaches to anticipate failure in advance of its occurrence is a cost and risk minimizing approach that is being implemented by most industries [34].

3.1.1. Artificial Neural Network (ANN)

A subcategory of statistical machine learning, neural network (NN), is often used in various kinds of prediction tasks. Artificial neural networks is the most commonly used branch of neural networks; they work very similarly to brain neurons. Due to their accuracy in predicting output over other methods of prediction of non-linear input variables, ANNs have recently been emerging as a forecasting solution.

In this study, a MATLAB computer program was employed to plan the best ANN structure. The information layer was identified with pulse current, pulse on-time, and voltage. The yield layer was compared to the MRR, TWR and R_a. In the proposed model, the data layer was identified with a hidden layer neuron and the concealed layer was related to yield layers. After expansive fundamentals and based on investigation of the network, the ANN model for the MRR, TWR, and R_a was created.

The ANN architecture is defined by the way in which the neurons are interconnected. The network is fed with a set of input–output pairs, and it is trained to reproduce the output. The structure of each ANN is represented as (i, j, k), where i expresses the number of nodes in the input layer, j the nodes in the hidden layer, and k the nodes in the output layer. In Figure 3, the typical structure of a multi-layer ANN model is presented. In this example a model of an ANN (3-10-3) structure is presented with three variables (T_{on}, I, and V) in the input layer, 10 nodes in the hidden layer, and 3 nodes (MRR, TWR, and R_a) in the output layer [35].

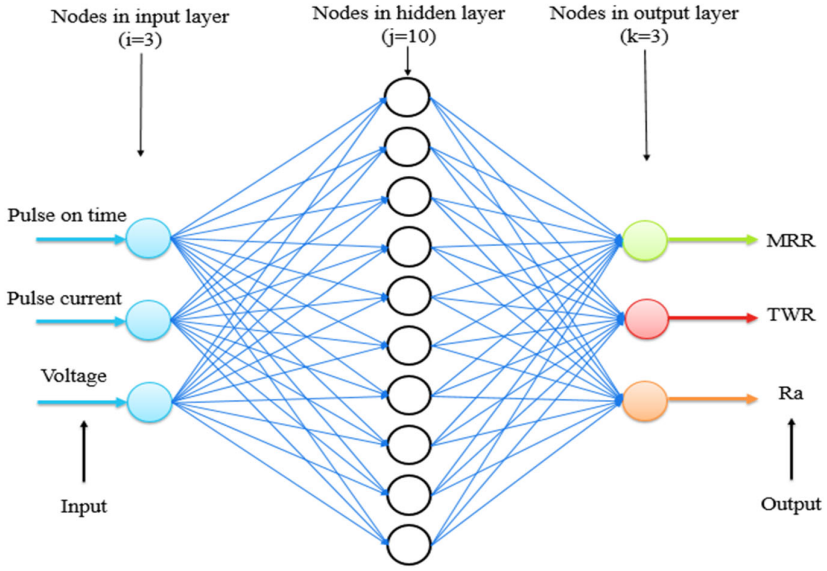

Figure 3. Typical structure of a multi-layer ANN model with 3 nodes in the input layer, 10 nodes in the hidden layer, and 3 nodes in the output layer.

In this investigation, the ANN prediction model is trained for each component using the Levenberg–Marquardt algorithm which shows a stable and a fast convergence. Figure 4 reveals the design of this ANN: 3 layers with full connection and 3 input nodes are logged into the input layer to describe 3 outputs. The input nodes include pulse-on time, pulse

current, and voltage. The output of this design is MRR, TWR, and R_a. Additionally, a total of seventy percent (70%) of the experimental data was used for training, with 15% used for validation and testing, respectively. The training algorithm used was the Levenberg–Marquardt algorithm [36].

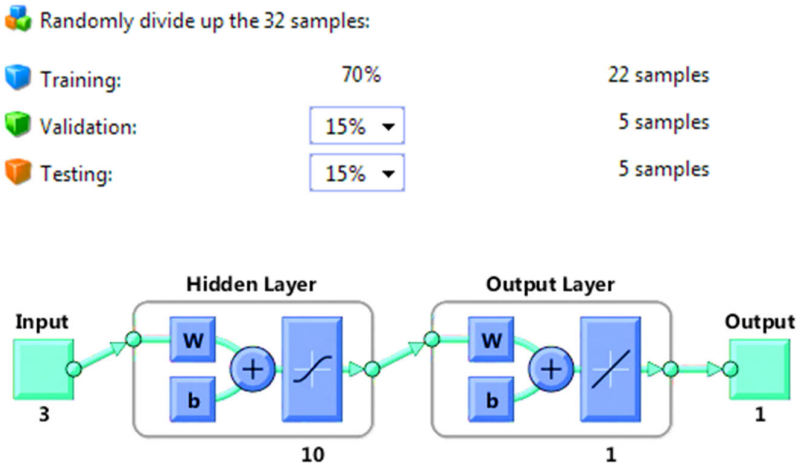

Algorithms	
Data Division	Random (dividerand)
Training	Levenberg–Marquardt (trainlm)
Performance	Mean Squared Error (mse)
Calculation	MEX

Figure 4. The schematic architecture of the ANN model.

Figure 5 shows the correlation of the RMSE error in both the validation and the training sets for the different numbers of hidden units after 100 iterations. The hidden layer with 10 neurons gave the minimum RMSE values for the training and testing sets. Figures 6–8 show the performance of the proposed ANN model (3LM10-3) for MRR, TWR, and R_a, respectively. These figures show the training, testing, and validation processes of the 3LM10-3 model starting at a large value and decreasing to a smaller value. The best training performances obtained were 1.5994 at the 22nd epoch, 0.1653 at the 4th epoch, and 0.074334 at the 3rd epoch, for MRR, TWR, and R_a, respectively. A minimum value of the MSE defines a good ANN model.

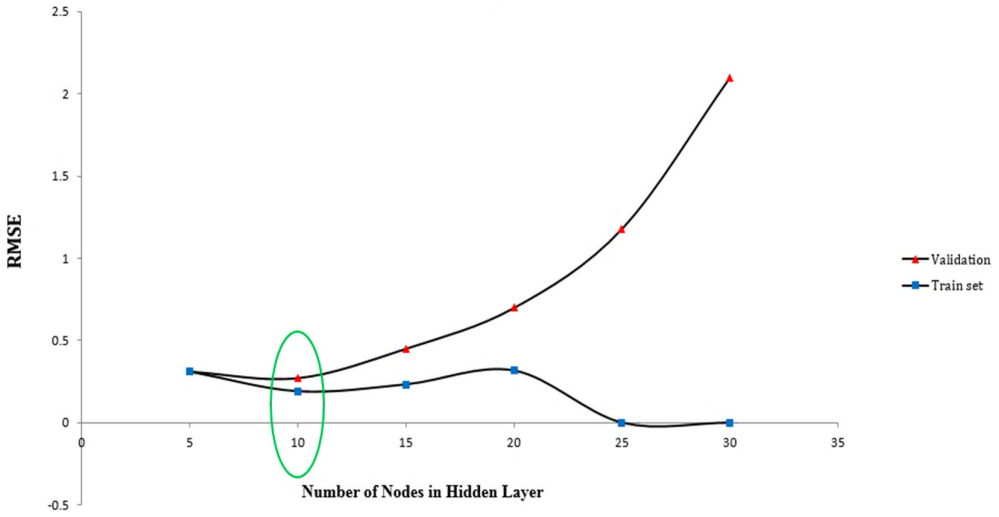

Figure 5. Root mean square error versus number of hidden units in both validation and training sets.

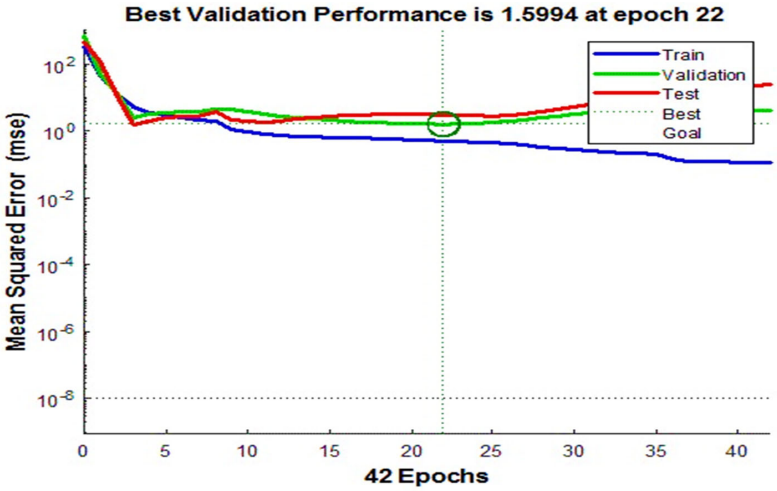

Figure 6. Performance of the 3LM10-3 model for MRR.

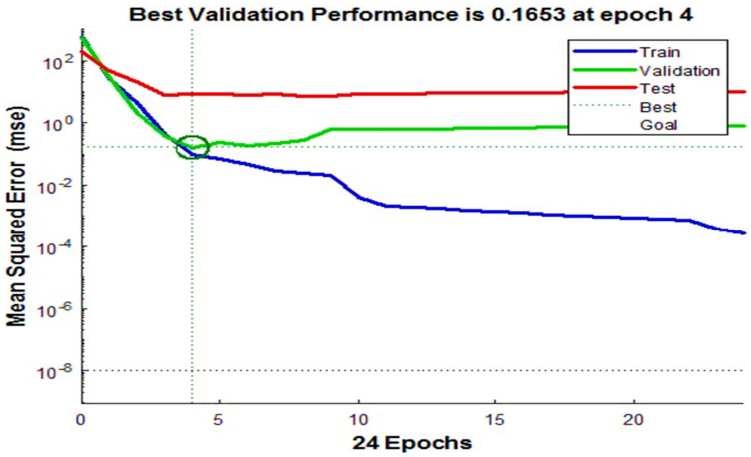

Figure 7. Performance of the 3LM10-3 model for TWR.

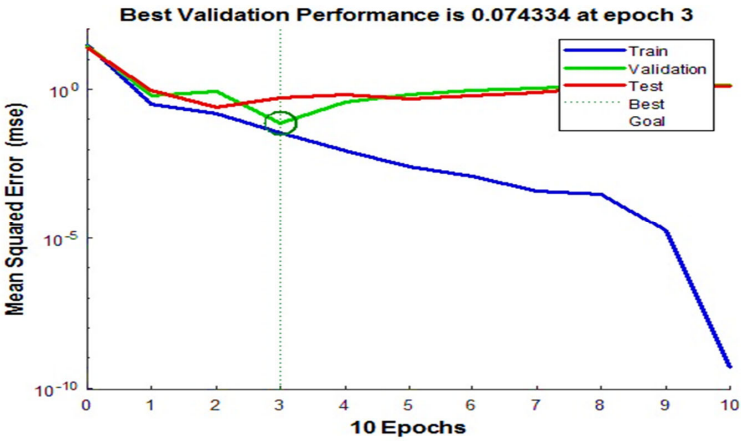

Figure 8. Performance of the 3LM10-3 model for R_a.

Figures 9–11 show the coefficient regression of training, testing, validation, and all the data from the 3LM10-3 model. These figures explain the correlation between the target (experimental data) and the ANN model output. The dashed line in each figure represents the targeted values. The best-fit linear regression line between the outputs and the targets is represented by a solid line. The values of coefficients for training, testing, validation, and all the data were found to be 0.99724, 0.99061, 0.98597, and 0.99415 for MRR; 0.99863,

0.96499, 0.99812, and 0.98535 for TWR; and 0.97594, 0.89775, 0.99113, and 0.95076 for R_a, respectively. The overall response with *R* close to 1 verified that training produced the optimal results. The root mean square error (RMSE) of the training model for MRR, TWR, and R_a are 1.03, 1.17, and 0.33, respectively.

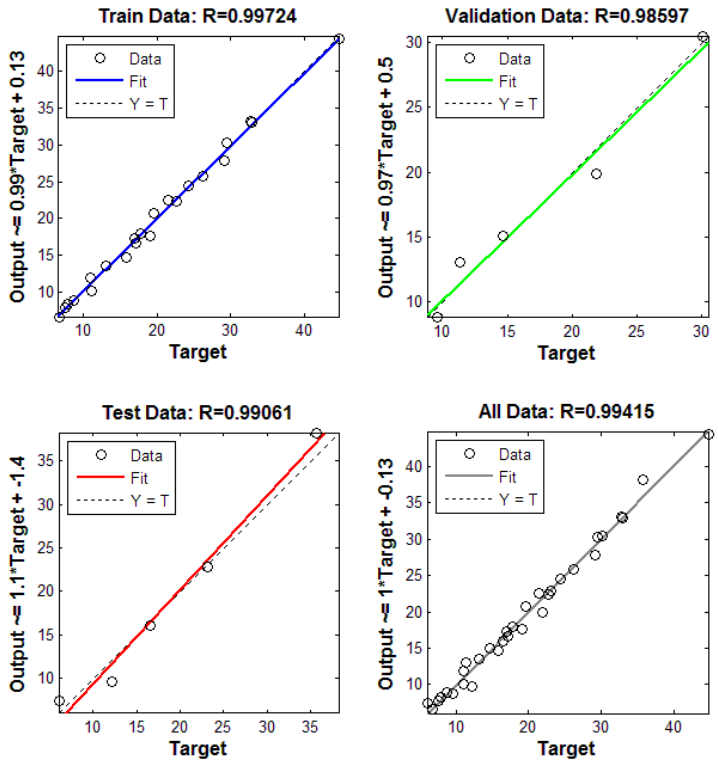

Figure 9. The plot of all data regression for data set of MRR.

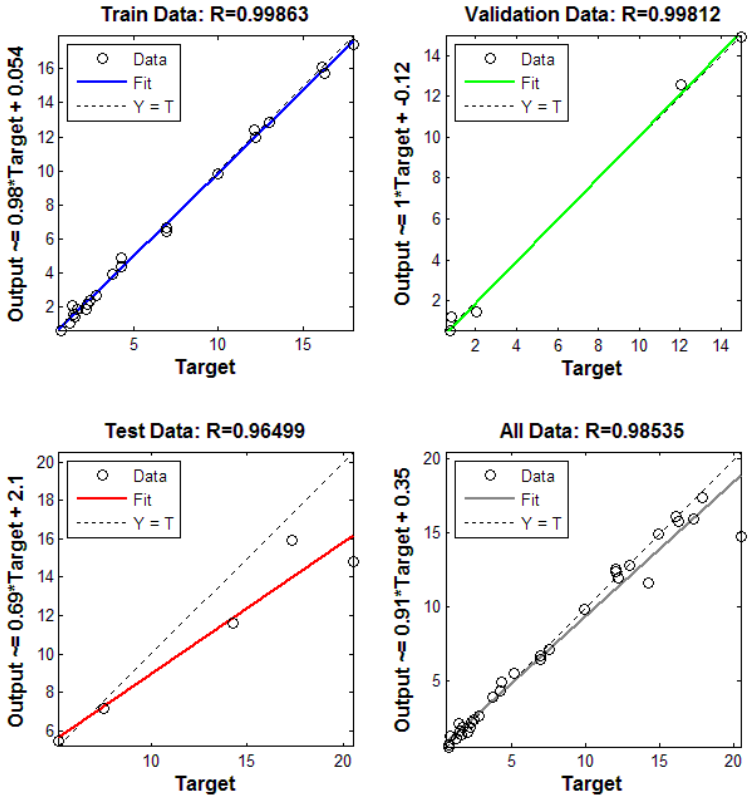

Figure 10. The plot of all data regression for the data set of TWR.

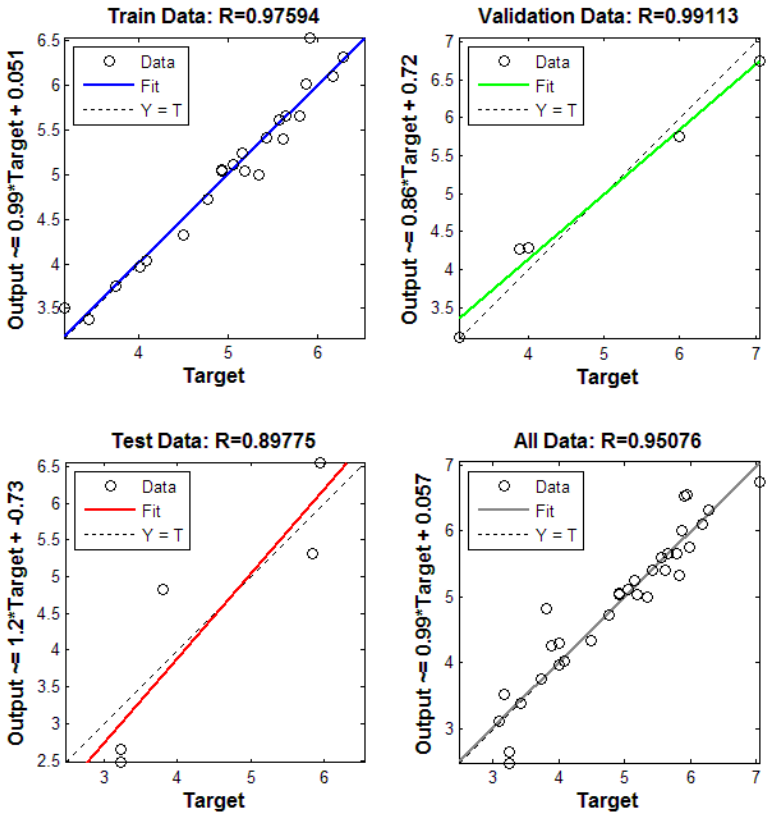

Figure 11. The plot of all data regression for the data set of R_a.

3.1.2. Adaptive Neural Fuzzy Inference System (ANFIS)

The word ANFIS means an adaptive neuro-fuzzy inference system that uses a specified input/output data collection; the ANFIS toolbox creates a fuzzy inference system (FIS), and its subscription includes calibrated (tuned) variables) either using a backpropagation method on its own or in combination with a least squares type approach. This modification allows the fuzzy structures to learn from the data they are processing. The neuro-adaptative learning approach works in a similar way to that of neural networks. Neuro-adaptative learning methods provide a mechanism for a fuzzy modeling system to learn details about data collection. The Mamdani fuzzy inference system's fundamental structure is a model that maps input features to input membership functions, input membership functions to principles, rules to a set of output features, output features to output membership functions, and output membership functions to a single-valued output or output-related decision. Such a system uses fixed membership functions that are chosen arbitrarily and a rule structure that is essentially predetermined by the user's interpretation of the characteristics of the variables in the model. The fuzzy inference style utilized in this paper contains three inputs, three MFs for every input, and two rules. The Takagi–Sugeno fuzzy design aimed to be consistent with the two IF rules constructed as follows [37]. The ANFIS utilized in this investigation was settled with MATLAB. Figure 12 demonstrates the view of the developed ANFIS model.

The planned ANFIS designs for the output parameters is shown in Figure 13. It includes 3 nodes in the input layer, 100 nodes in the hidden layer, and 3 nodes (MRR, TWR, and R_a) in the output layer. Figures 14–16 exhibit the contour and the 3D graph of MRR, TWR, and Ra values with different input parameters. The results of the graphs show that MRR increases with the increase in the pulse current and the pulse on-time. On the other hand, as the pulse current decreases, the MRR decreases. Figure 17 shows the graph of the estimated values versus the actual values for MRR, TWR, and R_a. The results prove that the estimated values are in good agreement with the actual responses. The root mean square error (RMSE) of the ANFIS training model for MRR, TWR, and R_a are 0.81, 0.28,

and 0.17, respectively. The precision of the ANFIS model relies on a couple of essential variables, which are listed in Table 3.

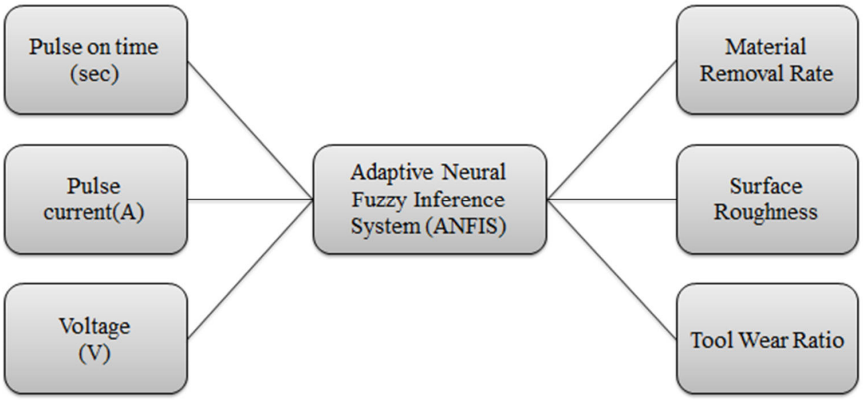

Figure 12. Observation of the established fuzzy model.

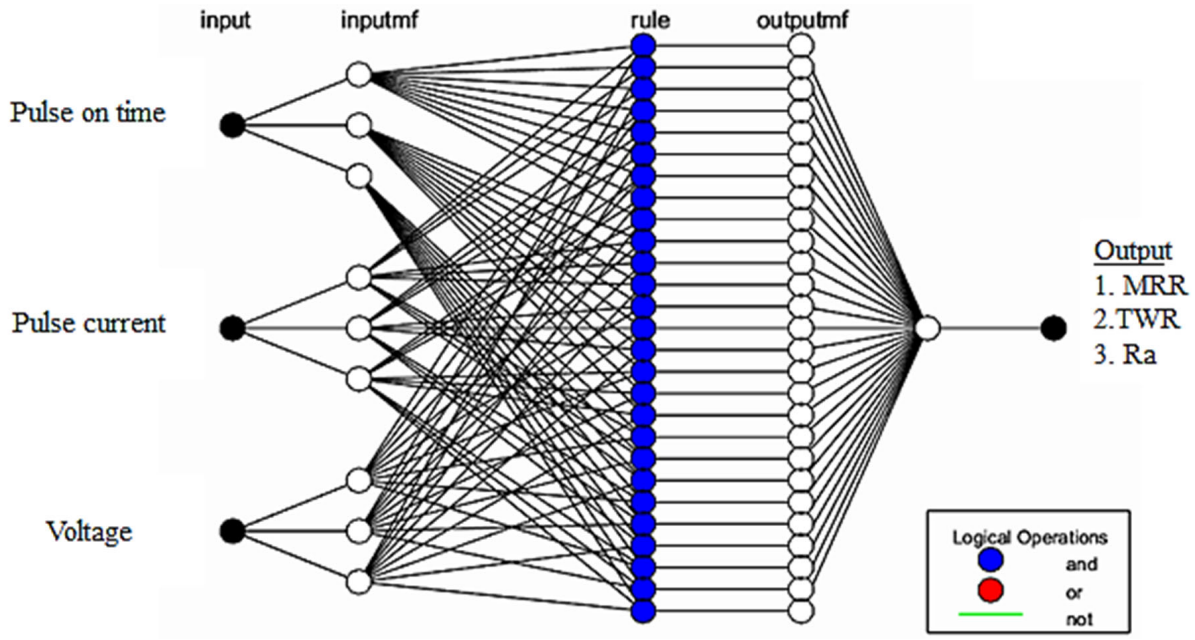

Figure 13. The design of the ANFIS model for output parameters (MRR, TWR, and R_a).

Table 3. ANFIS architecture and training parameters.

Number of nodes	78
Number of linear parameters	27
Number of nonlinear parameters	18
Total number of parameters	45
Number of training data pairs	32
Number of checking data pairs	5
Number of fuzzy rules	27

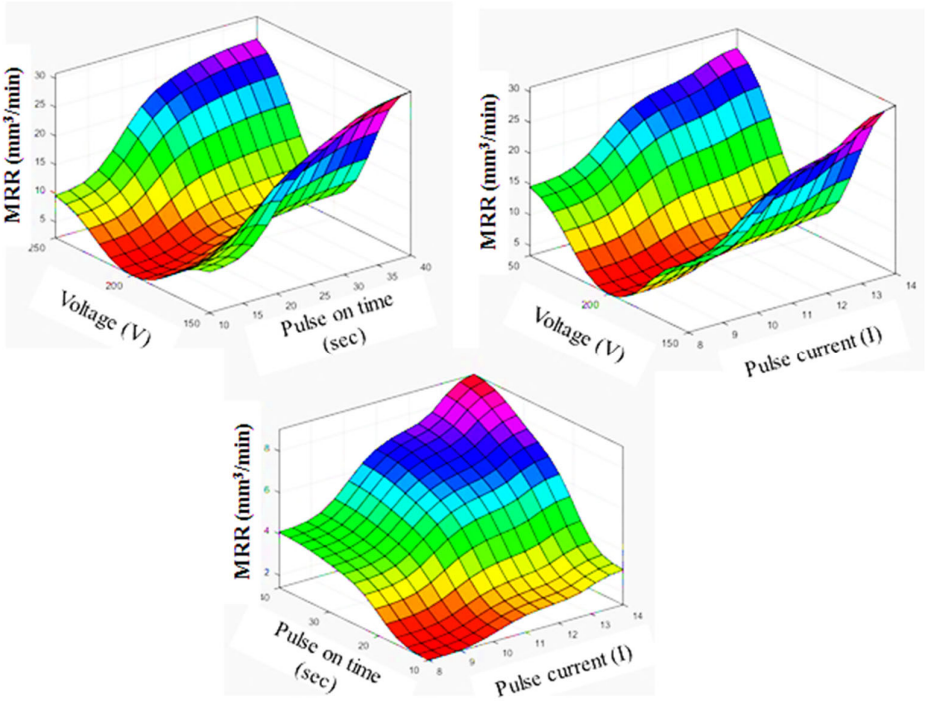

Figure 14. The 3D relations of input parameters versus MRR for ANFIS model.

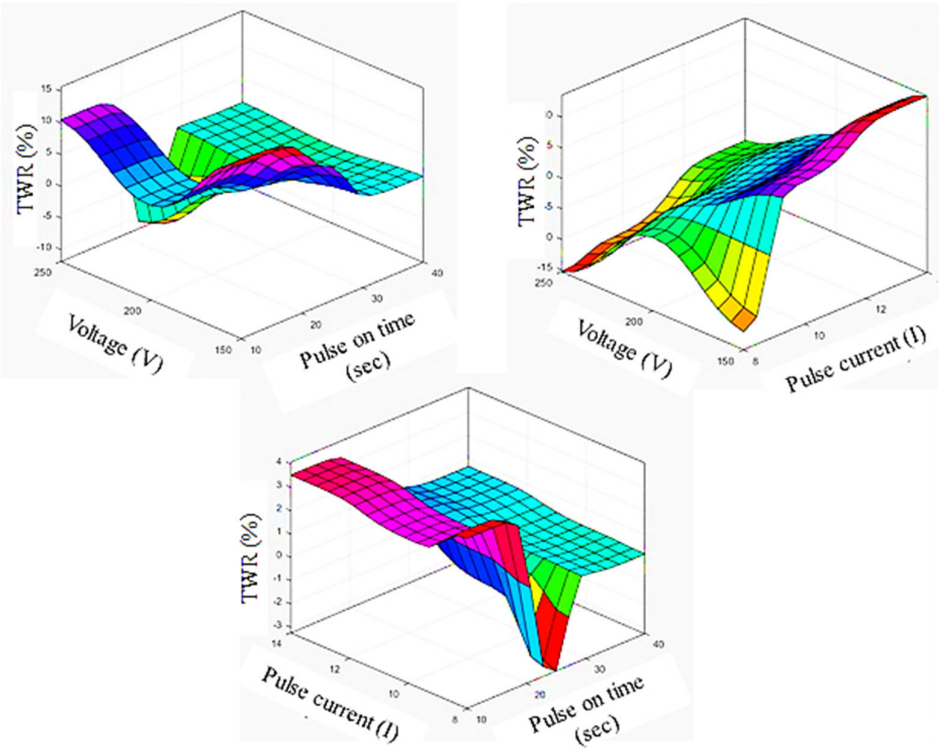

Figure 15. The 3D relations of input parameters versus TWR for ANFIS model.

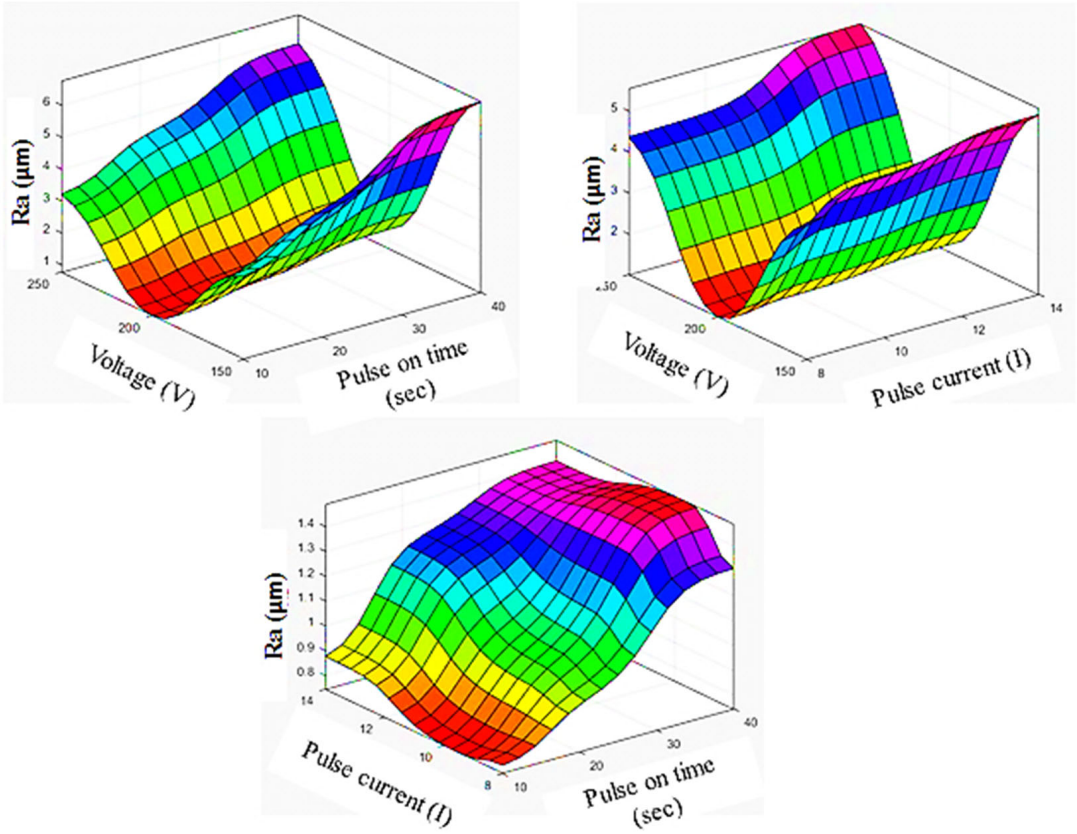

Figure 16. The 3D relations of input parameters versus R_a for ANFIS model.

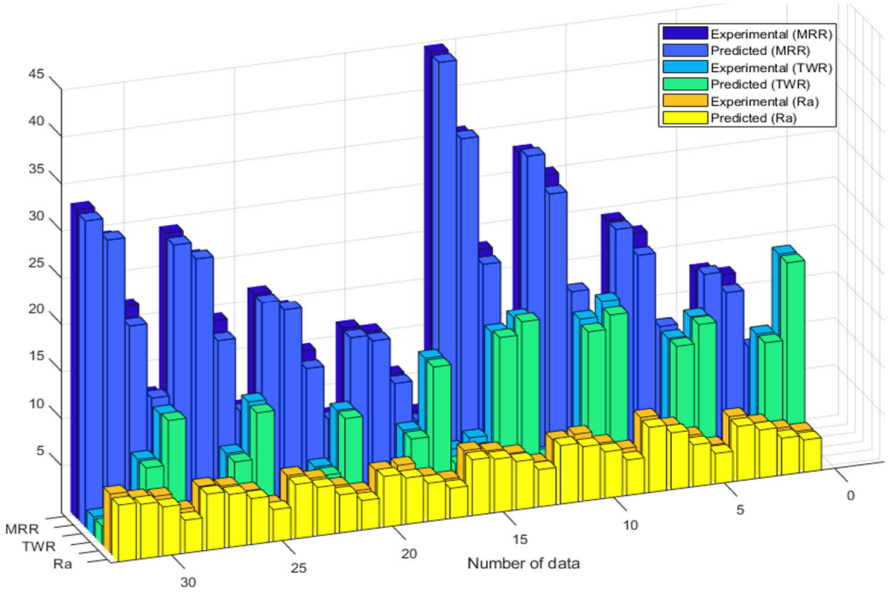

Figure 17. ANFIS results; estimated responses vs. actual values scheme for MRR, TWR, and R_a.

3.2. Prediction Error

The precision of the prediction model was evaluated by using the root mean square error (RMSE) [38]. The accompanying condition can be utilized to get the RMSE.

$$RMSE = \sqrt{\frac{1}{N}\sum_{i=1}^{N}(pi - qi)^2} \quad (3)$$

where N is the complete training data, p_i is the estimation of the deliberate information, and q_i is the worth, anticipated by the ANFIS model. The adequacy of the created model was checked by the mean square error (MSE), root mean square error (*RMSE*), and standard deviations [39], and it is depicted in Tables 4–6. From these evaluations, it very well may be surmised that the prompted model has the dynamically accurate expectation.

3.3. Prediction of Output Responses

With the help of an artificial neural network (ANN), an adaptive neural fuzzy inference system (ANFIS), and the prophetic value of MRR, TWR and R_a were detected for observation in training data sets as depicted in Tables 4–6. Two parameters such as MSE and RMSE were used to examine the outcome of models for the better judgment of the MRR, TWR, and R_a value obtained through the ANN and ANFIS methodologies. The values of the MSE and RMSE for all the models were specified in Table 7. The outcomes show that the actual responses are in near agreement with the predicted responses. The root mean square error (RMSE) of the ANN and the ANFIS models are 1.03 and 0.81 for MRR; 1.17 and 0.28 for TWR; and 0.33 and 0.17 for R_a, which proves that ANFIS models are relatively superior to other ML techniques.

Table 4. Testing the capability of all models in the prediction of MRR.

	Experimental Parameters			Expt	Model Prediction		Error	
No	**I**	**T_{on}**	**V**	**Value**	**ANN**	**ANFIS**	**ANN**	**ANFIS**
1	8	10	150	6.044916	7.40094	5.20004	1.356	−0.845
2	8	20	150	8.696462	8.885814	9.966221	0.189	1.2698
3	8	30	150	17.05669	16.69261	16.09935	−0.364	−0.957
4	8	40	150	17.77503	17.87653	18.35636	0.101	0.5813
5	10	10	150	7.911647	8.300831	7.214604	0.389	−0.697
6	10	20	150	11.34493	13.03521	13.3308	1.69	1.9859
7	10	30	150	22.64498	22.34559	21.27945	−0.299	−1.366
8	10	40	150	24.34266	24.50652	24.33714	0.164	−0.006
9	12	10	150	11.10143	10.14908	10.23128	−0.952	−0.87
10	12	20	150	16.91269	17.30969	18.34621	0.397	1.4335
11	12	30	150	30.0778	30.46354	29.01461	0.386	−1.063
12	12	40	150	32.78978	33.13807	33.32342	0.348	0.5336
13	14	10	150	13.11668	13.54476	13.44128	0.428	0.3246
14	14	20	150	23.10135	22.83831	22.47436	−0.263	−0.627
15	14	30	150	35.64444	38.20145	36.09756	2.557	0.4531
16	14	40	150	44.64781	44.32793	44.49635	−0.32	−0.151
17	8	10	250	6.712741	6.662043	6.701174	−0.051	−0.012
18	8	20	250	11.02284	11.93448	10.97197	0.912	−0.051
19	8	30	250	15.80746	14.71322	15.7947	−1.094	−0.013
20	8	40	250	16.53785	16.03618	16.43005	−0.502	−0.108
21	10	10	250	7.576641	7.825279	8.092684	0.249	0.516
22	10	20	250	14.66197	15.05229	13.7811	0.39	−0.881
23	10	30	250	19.60727	20.68079	20.3264	1.074	0.7191
24	10	40	250	21.47027	22.55168	21.42358	1.081	−0.047
25	12	10	250	9.611261	8.809756	10.18376	−0.802	0.5725
26	12	20	250	19.1213	17.64114	17.95628	−1.48	−1.165
27	12	30	250	26.23166	25.77989	27.03839	−0.452	0.8067
28	12	40	250	29.1648	27.87662	28.82355	−1.288	−0.341
29	14	10	250	12.20727	9.685567	12.79918	−2.522	0.5919
30	14	20	250	21.89337	19.84489	20.74241	−2.048	−1.151
31	14	30	250	29.43663	30.33535	30.26816	0.899	0.8315
32	14	40	250	32.8661	32.97477	32.59584	0.109	−0.27

Table 5. Testing the capability of all models in the prediction of TWR.

	Experimental Parameters			Expt	Model Prediction		Error	
No	**I**	**T_{on}**	**V**	**Value**	**ANN**	**ANFIS**	**ANN**	**ANFIS**
1	8	10	150	20.49628	14.80214	20.49113	−5.69	−0.005
2	8	20	150	12.22179	11.99425	12.21554	−0.23	−0.006
3	8	30	150	1.71064	1.828137	1.855931	0.117	0.1453
4	8	40	150	0.805808	1.21488	0.671929	0.409	−0.134
5	10	10	150	14.9604	14.91488	15.06815	−0.05	0.1077
6	10	20	150	12.98909	12.84186	13.06678	−0.15	0.0777
7	10	30	150	2.215157	1.868149	2.138513	−0.35	−0.077
8	10	40	150	1.295127	1.079804	1.138633	−0.22	−0.156
9	12	10	150	17.90438	17.42396	17.31107	−0.48	−0.593
10	12	20	150	16.25867	15.7496	15.8289	−0.51	−0.43
11	12	30	150	3.753688	3.902268	4.254516	0.149	0.5008
12	12	40	150	2.435521	2.355693	3.219124	−0.08	0.7836
13	14	10	150	17.32432	15.94907	17.81167	−1.38	0.4874
14	14	20	150	16.0907	16.09635	16.44482	0.006	0.3541
15	14	30	150	5.199727	5.471832	4.726387	0.272	−0.473
16	14	40	150	4.264924	4.352463	3.683061	0.088	−0.582
17	8	10	250	14.24802	11.59812	14.24613	−2.65	−0.002
18	8	20	250	6.914154	6.402733	6.91212	−0.51	−0.002
19	8	30	250	1.411702	2.085448	1.461996	0.674	0.0503
20	8	40	250	0.775119	0.532355	0.728759	−0.24	−0.046
21	10	10	250	9.954948	9.826657	10.00355	−0.13	0.0486
22	10	20	250	4.279131	4.879254	4.285975	0.6	0.0068
23	10	30	250	1.484691	1.580431	1.330647	0.096	−0.154
24	10	40	250	0.779914	0.638105	0.868602	−0.14	0.0887
25	12	10	250	12.07978	12.37901	11.83927	0.299	−0.241
26	12	20	250	6.939682	6.680634	6.937462	−0.26	−0.002
27	12	30	250	2.29648	2.173512	2.358917	−0.12	0.0624
28	12	40	250	1.554845	1.380158	1.789565	−0.17	0.2347
29	14	10	250	12.04724	12.57006	12.24898	0.523	0.2017
30	14	20	250	7.520435	7.134863	7.52897	−0.39	0.0085
31	14	30	250	2.790472	2.651723	2.588242	−0.14	−0.202
32	14	40	250	2.047492	1.477596	1.994939	−0.57	−0.053

Table 6. Testing the capability of all models in the prediction of R_a.

	Experimental Parameters			Expt	Model Prediction		Error	
No	**I**	**T_{on}**	**V**	**Value**	**ANN**	**ANFIS**	**ANN**	**ANFIS**
1	8	10	150	3.43	3.376873	3.439442	−0.053	0.0094
2	8	20	150	4.01	4.287986	3.929857	0.278	−0.08
3	8	30	150	4.92	5.05046	5.103606	0.1305	0.1836
4	8	40	150	5.91	6.52498	5.797063	0.615	−0.113
5	10	10	150	3.17	3.512229	3.245244	0.3422	0.0752
6	10	20	150	4.5	4.326987	4.45652	−0.173	−0.043
7	10	30	150	5.84	5.318601	6.03458	−0.521	0.1946
8	10	40	150	7.05	6.744532	6.920684	−0.305	−0.129
9	12	10	150	4.01	3.960998	3.763625	−0.049	−0.246
10	12	20	150	4.92	5.039596	4.945607	0.1196	0.0256
11	12	30	150	6.18	6.107069	5.791721	−0.073	−0.388
12	12	40	150	5.95	6.548194	6.222229	0.5982	0.2722
13	14	10	150	3.81	4.827091	3.973394	1.0171	0.1634
14	14	20	150	5.06	5.117459	5.14347	0.0575	0.0835
15	14	30	150	5.65	5.658762	5.693384	0.0088	0.0434
16	14	40	150	5.99	5.747169	5.939528	−0.243	−0.05
17	8	10	250	3.24	2.649677	3.218985	−0.59	−0.021

Table 6. *Cont.*

	Experimental Parameters			Expt	Model Prediction		Error	
No	**I**	**T_{on}**	**V**	**Value**	**ANN**	**ANFIS**	**ANN**	**ANFIS**
18	8	20	250	3.89	4.266676	4.068164	0.3767	0.1782
19	8	30	250	5.34	5.002421	4.93177	−0.338	−0.408
20	8	40	250	5.15	5.24454	5.401096	0.0945	0.2511
21	10	10	250	3.24	2.476626	3.14556	−0.763	−0.094
22	10	20	250	4.08	4.032333	4.054105	−0.048	−0.026
23	10	30	250	5.19	5.03863	5.163834	−0.151	−0.026
24	10	40	250	5.8	5.659738	5.782211	−0.14	−0.018
25	12	10	250	3.09	3.105256	3.414244	0.0153	0.3242
26	12	20	250	4.77	4.731091	4.889681	−0.039	0.1197
27	12	30	250	5.61	5.401034	5.632478	−0.209	0.0225
28	12	40	250	5.87	6.010513	5.973753	0.1405	0.1038
29	14	10	250	3.74	3.75692	3.522968	0.0169	−0.217
30	14	20	250	5.43	5.407616	5.227786	−0.022	−0.202
31	14	30	250	5.57	5.607572	5.82209	0.0376	0.2521
32	14	40	250	6.29	6.317659	6.05123	0.0277	−0.239

Table 7. Evaluation parameters performance table for MRR, TWR, and R_a.

Model	Training Set	
	Mean Squared Error (MSE)	**Root Mean Square Error (RMSE)**
Material Removal Rate Data Set (MRR)		
Artificial Neural Network	1.07	1.03
Adaptive Neural Fuzzy Inference System	0.67	0.81
Tool Wear Ratio (TWR)		
Artificial Neural Network	1.39	1.17
Adaptive Neural Fuzzy Inference System	0.08	0.28
Surface Roughness (R_a)		
Artificial Neural Network	0.11	0.33
Adaptive Neural Fuzzy Inference System	0.03	0.17

4. Conclusions

In the current investigation, two models—artificial neural network (ANN) and adaptive neuro-fuzzy inference system (ANFIS)—have been utilized to estimate the MRR, TWR, and R_a, in the EDM of AISI-D6 tool steel. The important conclusions of the study are summarized as follows:

(1) As the pulse current and pulse on-time increase, the material removal rate increases; and, conversely, it decreases as the voltage increases, especially when the pulse current is above 30 A.

(2) The tool wear ratio increases as the pulse current increases, it decreases when the voltage increases; and as the impact on-time increases, it decreases in contrast to the increase in the metal removal rate.

(3) In terms of roughness, surface quality improves with decreasing pulse current and pulse on-time, and it improves as the voltage is increased.

(4) Both the accuracy of prediction and the suitability for use of these models are considered to support the forecast. The results indicate that the ANFIS approach is relatively superior to other ML techniques, providing more reliable and accurate results in terms of lower RMSE (0.81, 0.28, and 0.17) for output parameter requirements in electric discharge machining.

(5) The trends presented in this study are expected to act as guidelines for users to set the parameters in order to achieve their desired objective. Furthermore, from the

above findings, it follows that the effect of input parameters on various performance measures of the process are opposing in nature. Therefore, to acquire a trade-off among all of the considered measures, the parameters should be set to intermediate values of the settings employed in this study.

(6) In the future, hybrid models can be applied to further increase the accuracy of forecasts. Hybrid models combine machine learning techniques with optimization algorithms. They are more powerful than single models as they commonly incorporate the advantages and they compensate for the weaknesses of the individual techniques involved, improving forecasting accuracy. Hybrid models can be created with one or more phases, corresponding to different problem-solving goals.

Author Contributions: H.H.P., Conceptualization, Methodology, Formal Analysis, Writing—Original Draft; M.J., Methodology, Investigation, Formal Analysis, Review and Editing, Project administration; V.M.K., Conceptualization, Methodology, Investigation, Validation, Review and Editing; R.V.B., Conceptualization, Methodology, Validation, Writing—Original Draft. All authors have read and agreed to the published version of the manuscript.

Funding: This research received no external funding.

Institutional Review Board Statement: Not applicable.

Informed Consent Statement: Not applicable.

Data Availability Statement: Not applicable.

Conflicts of Interest: The authors declare no conflict of interest.

References

1. Barenji, R.V.; Pourasl, H.H.; Khojastehnezhad, V.M. Electrical discharge machining of the AISI D6 tool steel: Prediction and modeling of the material removal rate and tool wear ratio. *Precis. Eng.* **2016**, *45*, 435–444. [CrossRef]
2. Țîțu, A.M.; Vizureanu, P.; Țîțu, Ș.; Sandu, A.V.; Pop, A.B.; Bucur, V.; Ceocea, C.; Boroiu, A. Experimental Research on the Cutting of Metal Materials by Electrical Discharge Machining with Contact Breaking with Metal Band as Transfer Object. *Materials* **2020**, *13*, 5257. [CrossRef] [PubMed]
3. Boujelbene, M.; Bayraktar, E.; Tebni, W.; Salem, S.B. Influence of machining parameters on the surface integrity in electrical discharge machining. *Arch. Mater. Sci. Eng.* **2009**, *37*, 110–116.
4. Pradhan, D.; Jayswal, S. Behaviour of copper and aluminium electrodes on EDM of EN-8 alloy steel. *Int. J. Eng. Sci. Technol.* **2011**, *3*, 5492–5499.
5. Amorim, F.L.; Weingaertner, W.L. The behavior of graphite and copper electrodes on the finish die-sinking electrical discharge machining (EDM) of AISI P20 tool steel. *J. Braz. Soc. Mech. Sci. Eng.* **2007**, *29*, 366–371. [CrossRef]
6. Jafferson, J.; Hariharan, P. Machining performance of cryogenically treated electrodes in microelectric discharge machining: A comparative experimental study. *Mater. Manuf. Processes* **2013**, *28*, 397–402. [CrossRef]
7. Singh, B.; Misra, J. Surface finish analysis of wire electric discharge machined specimens by RSM and ANN modeling. *Measurement* **2019**, *137*, 225–237. [CrossRef]
8. Vishnu, P.; Kumar, N.S.; Manohar, M. Performance prediction of electric discharge machining of Inconel-718 using artificial neural network. *Mater. Today Proc.* **2018**, *5*, 3770–3780. [CrossRef]
9. Tebni, W.; Boujelbene, M.; Bayraktar, E.; Salem, S.B. Parametric approach model for determining electrical discharge machining (EDM) conditions: Effect of cutting parameters on the surface integrity. *Arab. J. Sci. Eng.* **2009**, *34*, 101–114. [CrossRef]
10. Kiyak, M.; Çakır, O. Examination of machining parameters on surface roughness in EDM of tool steel. *J. Mater. Processing Technol.* **2007**, *191*, 141–144. [CrossRef]
11. Muthuramalingam, T.; Mohan, B. Influence of discharge current pulse on machinability in electrical discharge machining. *Mater. Manuf. Processes* **2013**, *28*, 375–380. [CrossRef]
12. Chandramouli, S.; Shrinivas Balraj, U.; Eswaraiah, K. Optimization of electrical discharge machining process parameters using Taguchi method. *Int. J. Adv. Mech. Eng.* **2014**, *4*, 425–434.
13. Kibria, G.; Sarkar, B.; Pradhan, B.; Bhattacharyya, B. Comparative study of different dielectrics for micro-EDM performance during microhole machining of Ti-6Al-4V alloy. *Int. J. Adv. Manuf. Technol.* **2010**, *48*, 557–570. [CrossRef]
14. Jeykrishnan, J.; Ramnath, B.V.; Akilesh, S.; Kumar, R.P. Optimization of process parameters on EN24 tool steel using Taguchi technique in electro-discharge machining (EDM). In Proceedings of the IOP Conference Series: Materials Science and Engineering, Bangalore, India, 14–16 July 2016; IOP Publishing: Bristol, UK, 2016; Volume 1, p. 12022.
15. Yongfeng, G.; Yerui, F.; Li, W.; Kelie, D.; Changjin, M.; Lin, T. Experimental Investigation of EDM Parameters for ZrB2-SiC Ceramics Machining. *Procedia CIRP* **2018**, *68*, 46–51. [CrossRef]

16. Marafona, J.; Wykes, C. A new method of optimising material removal rate using EDM with copper–tungsten electrodes. *Int. J. Mach. Tools Manuf.* **2000**, *40*, 153–164. [CrossRef]
17. Her, M.-G.; Weng, F.-T. A study of the electrical discharge machining of semi-conductor $BaTiO_3$. *J. Mater. Processing Technol.* **2002**, *122*, 1–5. [CrossRef]
18. Shrivastava, P.K.; Dubey, A.K. Intelligent modeling and multiobjective optimization of electric discharge diamond grinding. *Mater. Manuf. Processes* **2013**, *28*, 1036–1041.
19. Baraskar, S.S.; Banwait, S.; Laroiya, S. Multiobjective optimization of electrical discharge machining process using a hybrid method. *Mater. Manuf. Processes* **2013**, *28*, 348–354. [CrossRef]
20. Raju, R.; Manikandan, N.; Palanisamy, D.; Arulkirubakaran, D.; SambathKumar, S.; Prakash, P.B. Optimization of process parameters in electrical discharge machining of haste alloy C276 using Taguchi's method. *Mater. Today Proc.* **2018**, *5*, 14432–14439. [CrossRef]
21. Basha, S.K.; Raju, M.J.; Kolli, M. Experimental study of electrical discharge machining of inconel X-750 using tungsten-copper electrode. *Mater. Today Proc.* **2018**, *5*, 11622–11627. [CrossRef]
22. Tsai, K.-M.; Wang, P.-J. Semi-empirical model of surface finish on electrical discharge machining. *Int. J. Mach. Tools Manuf.* **2001**, *41*, 1455–1477. [CrossRef]
23. Choudhary, R.; Singh, G. Effects of process parameters on the performance of electrical discharge machining of AISI M42 high speed tool steel alloy. *Mater. Today Proc.* **2018**, *5*, 6313–6320. [CrossRef]
24. Singh, N.K.; Pandey, P.M.; Singh, K. A semi-empirical model to predict material removal rate during air-assisted electrical discharge machining. *J. Braz. Soc. Mech. Sci. Eng.* **2019**, *41*, 122. [CrossRef]
25. Al-Ghamdi, K.; Taylan, O. A comparative study on modelling material removal rate by ANFIS and polynomial methods in electrical discharge machining process. *Comput. Ind. Eng.* **2015**, *79*, 27–41. [CrossRef]
26. Singh, N.K.; Singh, Y.; Kumar, S.; Sharma, A. Predictive analysis of surface roughness in EDM using semi-empirical, ANN and ANFIS techniques: A comparative study. *Mater. Today Proc.* **2019**, *25*, 735–741. [CrossRef]
27. Bobbili, R.; Madhu, V.; Gogia, A. Modelling and analysis of material removal rate and surface roughness in wire-cut EDM of armour materials. *Eng. Sci. Technol. Int. J.* **2015**, *18*, 664–668. [CrossRef]
28. Singh, N.K.; Singh, Y. Experimental Investigation and Modeling of Surface Finish in Argon-Assisted Electrical Discharge Machining Using Dimensional Analysis. *Arab. J. Sci. Eng.* **2019**, *44*, 5839–5850. [CrossRef]
29. Țîțu, A.M.; Sandu, A.V.; Pop, A.B.; Țîțu, Ș.; Frățilă, D.N.; Ceocea, C.; Boroiu, A. Design of experiment in the milling process of aluminum alloys in the aerospace industry. *Appl. Sci.* **2020**, *10*, 6951. [CrossRef]
30. Pourasl, H.H.; Barenji, R.V.; Khojastehnezhad, V.M. *Elucidating the Effect of Electrical Discharge Machining Parameters on the Surface Roughness of Aisi D6 Tool Steel Using Response Surface Method*; NISCAIR-CSIR: New Delhi, India, 2017.
31. Alpaydin, E. *Introduction to Machine Learning*; MIT Press: Cambridge, MA, USA, 2020.
32. Deng, L.; Yu, D. Deep learning: Methods and applications. *Found. Trends®Signal Processing* **2014**, *7*, 197–387. [CrossRef]
33. Wuest, T.; Weimer, D.; Irgens, C.; Thoben, K.-D. Machine learning in manufacturing: Advantages, challenges, and applications. *Prod. Manuf. Res.* **2016**, *4*, 23–45. [CrossRef]
34. Kashyap, P. Industrial applications of machine learning. In *Machine Learning for Decision Makers*; Springer: Berlin/Heidelberg, Germany, 2017; pp. 189–233.
35. Antonopoulos, V.Z.; Papamichail, D.M.; Aschonitis, V.G.; Antonopoulos, A.V. Solar radiation estimation methods using ANN and empirical models. *Comput. Electron. Agric.* **2019**, *160*, 160–167. [CrossRef]
36. Khojastehnezhad, V.M.; Pourasl, H.H.; Bahrami, A. Estimation of mechanical properties of friction stir processed al 6061/al2o3-tib2 hybrid metal matrix composite layer via artificial neural network and response surface methodology. *Proc. Inst. Mech. Eng. Part L J. Mater. Des. Appl.* **2021**, *235*, 2720–2736. [CrossRef]
37. Jang, J.-S. ANFIS: Adaptive-network-based fuzzy inference system. *IEEE Trans. Syst. Man Cybern.* **1993**, *23*, 665–685. [CrossRef]
38. Unune, D.R.; Mali, H.S. Artificial neural network–based and response surface methodology–based predictive models for material removal rate and surface roughness during electro-discharge diamond grinding of Inconel 718. *Proc. Inst. Mech. Eng. Part B J. Eng. Manuf.* **2016**, *230*, 2082–2091. [CrossRef]
39. Singh, N.K.; Kumar, S.; Singh, Y.; Sharma, V. Predictive analysis of surface finish in gas-assisted electrical discharge machining using statistical and soft computing techniques. *Surf. Rev. Lett.* **2019**, *27*, 1950126. [CrossRef]